Numerical Investigation of a Generic Rocket Model with Heated Plumes at Ma = 3

By S. Stephan†, R. Radespiel†, K. Oßwald‡ AND P. Birken¶

†Institute of Fluid Mechanics, Technische Universität Braunschweig, Hermann-Blenk-Str. 37, 38108 Braunschweig
‡Institute of Aerodynamics and Flow Technology, Deutsches Zentrum für Luft- und Raumfahrt (DLR), Bunsenstr. 10, 37073 Göttingen
¶Institut für Mathematik, Universität Kassel, Heinrich Plett Str. 40, 34132 Kassel

Afterbody flow phenomena represent a major source of uncertainties in the design of a space launcher. Hence, there is a demand for measuring and computing such flows. As a new approach there is a jet simulation facility integrated into a $Ma = 3$ supersonic wind tunnel. This jet simulation facility resembles an Ariane 5 European launcher at an altitude of $25km$. The computations done in this work are helpful to understand processes in the new jet simulation facility. The numerical simulations can be compared to planned experiments in the future.

1. Introduction

The interest in jet simulations is motivated by the need for experimental data in the area of afterbody flow phenomena. During atmospheric rocket flights there are a multitude of interactions between free stream and jet. These interactions influence the aerodynamic and thermal loads. While a number of investigations are reported in the literature on missiles, the literature on launchers with jet simulation is sparse. For example Peters [1, 2] researched the effect of the boattail drag for different jet simulation parameters by variation of the boattail, the nozzle exit to throat ratio, the jet temperature and the gas composition. Kumar [3] presented investigations in boattail separated flows relevant to launch vehicle configurations. This included mean and fluctuation pressure measurements. The investigations were performed at transonic speeds ranging from $Ma = 0.7 to 1.2$ and various boattail angles and nozzle diameters. Investigations of the Ariane 5 European launcher afterbody at a scale of 0.01 have been conducted by Reijasse [4]. The first stage including the center engine and boosters was studied in a blow down wind tunnel at $Ma = 4$. The jet was simulated with cold high pressure air, which was expanded to resemble flight at an altitude of $30km$. As a result the complex flow field consisting of supersonic, subsonic and reverse flows was determined.
For experimental research there is a new jet simulation facility at the Institute of Fluid Mechanics in Braunschweig [5]. From this facility there are measurements at free stream Mach number $Ma = 5.9$ now available. In the new DFG TRR 40 funding period this jet simulation facility will be used for research in supersonic flows at a free stream Mach number $Ma = 3$. In different experiments jet simulation will be performed with air and helium. The advantage to use helium is to get a similar velocity ratio between plume and ambient flow to the real velocity ratio observed along the Ariane 5 trajectory. The experiments will include PIV, Schlieren pictures and pressure measurements. The exper-

	$wind\ tunnel$	$Ariane\ 5\ trajectory$
Ma_∞ [-]	3	3
p_∞ [bar]	0.041	0.027
p_t [bar]	1.52	0.98
T_∞ [K]	101.8	216
T_t [K]	285	605

TABLE 1. Freestream conditions.

imental program is to be accompanied by flow simulations of the generic rocket model with helium and air exhaust at various total temperatures and total pressures. Numerical simulations for these cases are helpful to understand processes in the extended jet simulation facility, and to compare the experimental data with the numerical simulations. The numerical simulation data are also helpful to correct optical errors of the PIV measurements. These optical errors are caused by the high density gradients within the plume flow.

2. Jet Simulation

For simulating rocket afterbody flows in wind tunnel facilities it is important to reproduce the major rocket plume flow parameters. A review of various techniques for simulation of jet exhaust in ground testing facilities is given by Pindzola [6]. The scaling of the rocket plume for the jet simulation facility used in the present work is based on discussions with industry in rocket propulsion [7]. The launcher to be scaled is the Ariane 5 with a Vulcain 2 rocket motor at an altitude of $25km$. The free stream conditions at flight and in the wind tunnel are shown in Table 1.

The easiest approach would be a geometric scaling, but for wind tunnel experiments that is very difficult approach. Rocket motors used in launchers have hot rocket plumes with total temperatures up to $3500K$. This high temperature would create extreme heat loads on the wind tunnel models and limit the use of sensors. Also the infrastructure cost are extremely high. Hence jet simulations in wind tunnels usually employ cold plumes. But for physics based ground simulation two major afterbody flow mechanisms are important and should be considered. One mechanism is flow displacement by plume shape. The plume shape affects the positions of the shear layer and the plume shock. It mainly depends on the ratio of nozzle exit pressure to static pressure in the free-stream p_{jet}/p_∞. The second mechanism is flow entrainment into the plume. The entrainment describes the effect of the shear layer to entrain gas from the base flow. Entrainment results from turbulent mixing and this is associated with the large turbulent structures in the afterbody flow. Simulation of turbulent mixing is therefore needed to represent buffet flow phenomena at the rocket afterbody. Any differences between wind tunnel and rocket operation plume conditions will affect the similarity parameters for entrainment. This may be represented by the velocity ratio $(u_{max} - u_\infty)/u_{max}$. The maximum velocity $u_{max} = [(2 \cdot \gamma)/(\gamma - 1)(\Re \cdot T_t)/M_{Mol}]^{-1/2}$ depends on the molar massM_{Mol}, the specific heat ratio γ and the total temperature T_t. Therefore by changing the gas composition the velocity can be modified. The maximum velocity for the Vulcain 2 (H_2/O_2 combustion; $\gamma = 1.2$; $M_{Mol} = 13.5g/mol$) is $u_{max,Vulcain2} = 5086m/s$ at $T_t = 3500K$. Heated air

$working\ gas$ [−]	$p_{t,SC}$ $[bar]$	$T_{t,SC}$ $[K]$	$\rho_{t,SC}$ $[kg/m^3]$	p_{jet}/p_∞ [−]	$\frac{(u_{max}-u_\infty)}{u_{max}}$ [−]
air	3.55	285	4.34	5	0.20
air	3.55	620	2.00	5	0.45
helium	3.45	285	0.58	5	0.65
helium	3.45	540	0.31	5	0.74
helium	3.45	620	0.27	5	0.76
helium	3.45	800	0.21	5	0.79

TABLE 2. Varied jet flow parameters.

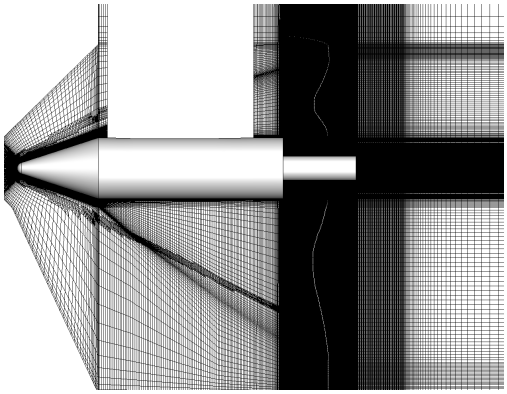

FIGURE 1. Computational domain.

($\gamma = 1.4; M_{Mol} = 29g/mol$) reaches 25% and heated helium ($\kappa = 1.67; M_{Mol} = 4g/mol$) 56% of $u_{max,Vulcain2}$ at $T_t = 800K$.

3. Setup

3.1. *Model and Flow Parameters*

The used generic rocket model resembles the European Ariane 5 launcher including the Vulcain 2 rocket engine. The main body is represented by a blunted cone with a nose radius of $10mm$ and a cone angle of $36°$ followed by a cylindrical part wit a diameter of $D = 108mm$. At the rocket base a TIC-nozzle (truncated ideal nozzle contour) is added. Two types of nozzle are needed, one if air is used as working gas and a other one for helium. Table 2 shows the important parameter total pressure in the settling chamber, $p_{t,SC}$, total temperature in the settling chamber, $T_{t,SC}$, total density in the settling chamber, $\rho_{t,SC}$ and the jet simulation parameters, p_{jet}/p_∞ and $(u_{max}-u_\infty)/u_{max}$ for the computed cases.

3.2. *Numerical Setup*

In this study three dimensional Reynolds-Averaged Navier-Stokes equations (RANS) solutions are computed and analysed. The DLR-TAU code with the one-equation Spalart-Allmaras turbulence model was used. For the computations a given grid was used [8, 9]. The computational domain is a 180 ° part of the geometry. The model symmetry is used to reduce computational cost. The structured grid consists of about 11 million cells. The

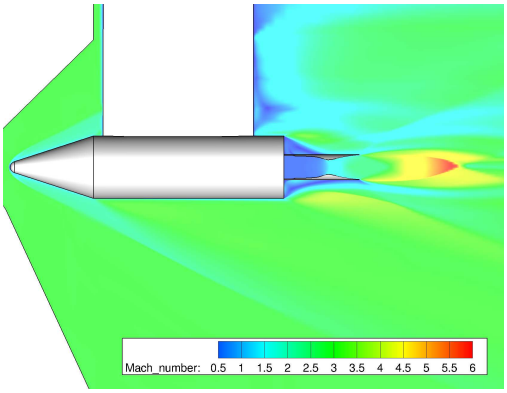

FIGURE 2. Mach number field in the symmetry plane for the cold air exhaust.

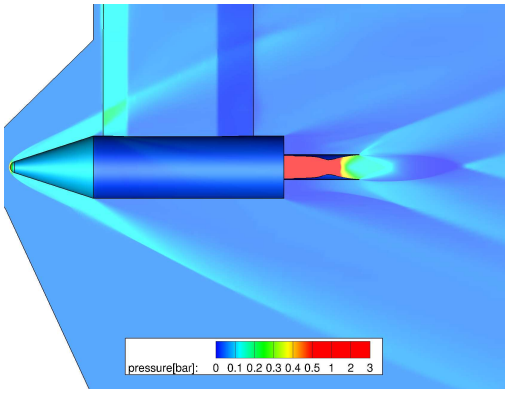

FIGURE 3. Pressure field in the symmetry plane for the cold air exhaust.

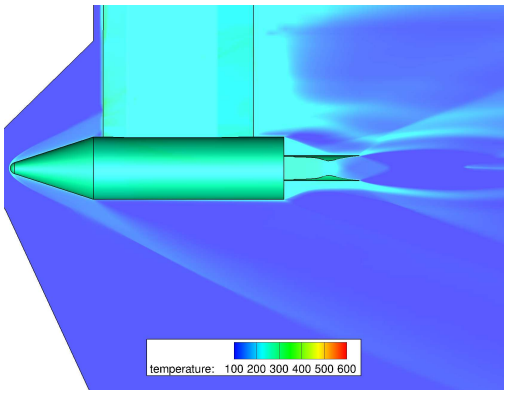

FIGURE 4. Temperature field in the symmetry plane for the cold air exhaust.

grid is adapted at the Mach 3 bow shock. Figure 1 shows a cut through the symmetry plane of the domain.

4. Numerical Results

In this section first results are shown. Unfortunately not all computations are completed yet. So we can only present the air exhaust results here. The overall flow topology in the symmetry plane is given by the mean Mach number distribution, the mean pressure distribution and the mean temperature distribution. The freestream Mach number is $Ma_\infty = 3$, the freestream total pressure $p_{t,\infty} = 1.52bar$ and the freestream total temperature is $T_{t,\infty} = 285K$.

4.1. *Cold Air Exhaust*

For the cold air exhaust the jet Mach number is $Ma_{jet} = 2.5$, total pressure is $p_{t,jet} = 3.55bar$ and the total temperature is $T_{t,jet} = 285K$. Figure 2 shows the mean Mach number distribution in the symmetry plane. It shows the bow shock in front of the model nose. This shock is conical along the cone. The support of the model has an influence on the whole afterbody flow field. Figure 3 shows the pressure distribution in the symmetry plane. The pressure in the jet settling chamber is much higher than the freestream

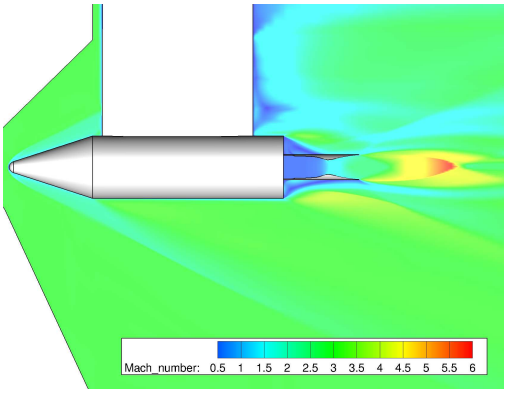

FIGURE 5. Mach number field in the symmetry plane for the heated air exhaust.

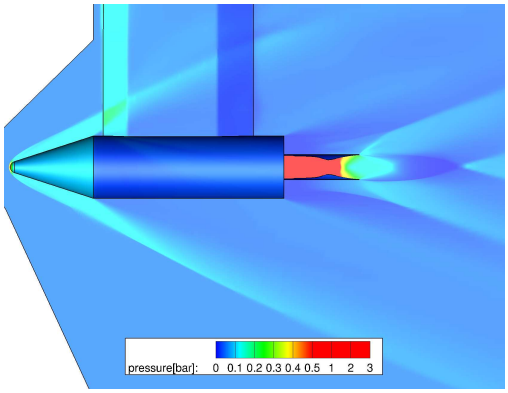

FIGURE 6. Pressure field in the symmetry plane for the heated air exhaust.

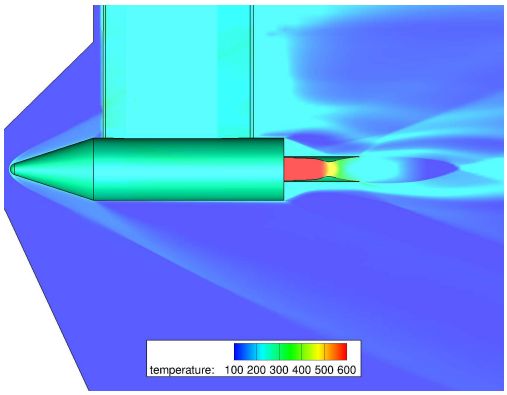

FIGURE 7. Temperature field in the symmetry plane for the heated air exhaust.

pressure. The jet is slightly underexpanded. Figure 4 shows the temperature distribution in the symmetry plane. The jet exit temperature and the freestream temperature are rather similar.

4.2. *Heated Air Exhaust*

For the heated air exhaust the jet Mach number is $Ma_{jet} = 2.5$, total pressure is $p_{t,jet} = 3.55bar$ and the total temperature is $T_{t,jet} = 620K$. Figure 5 shows the mean Mach number distribution, Figure 6 shows the pressure distribution and Figure 7 shows the temperature distribution in the symmetry plane. The flow field upstream the rocket base is rather similar to the cold jet case. Downstream the rocket base some differences are observed. These differences are caused by a higher jet temperature and therefore a higher jet velocity. Figure 8 shows the pressure coefficient c_p along the rocket base (opposing the sting support). The behavior of the curves are similar but for the heated air exhaust the c_p values are lower. This indicates that the outer flow turning towards the nozzle fairing is larger, for the heated air case. Figure 9 shows the pressure coefficient c_p along the nozzle fairing beginning from the rocket base ($x/D = 0$). Again the behavior is, quite similar. While at the rocket base the pressure coefficient for the heated air exhaust is smaller than the for the cold air exhaust, there is a large pressure rise towards the nozzle exit plane. Figure 10 shows the velocity ratio u/u_∞ in the symmetry plane

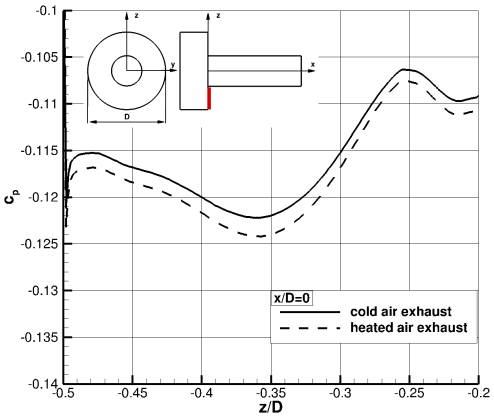

FIGURE 8. Pressure coefficient c_p distribution along the rocket base ($x/D = 0$) in the symmetry plane.

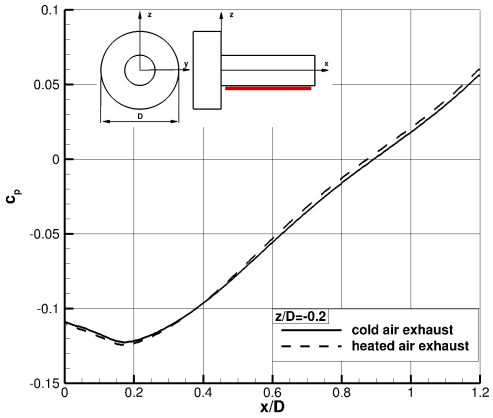

FIGURE 9. Pressure coefficient c_p distribution along the nozzle fairing ($z/D = -0.2$) in the symmetry plane.

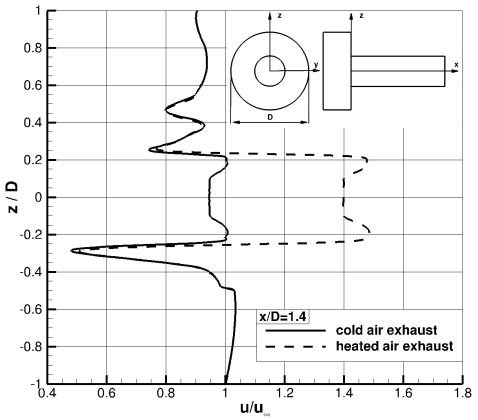

FIGURE 10. Velocity ratio $u/u\infty$ distribution behind the nozzle exit ($x/D = 1.4$) in the symmetry plane.

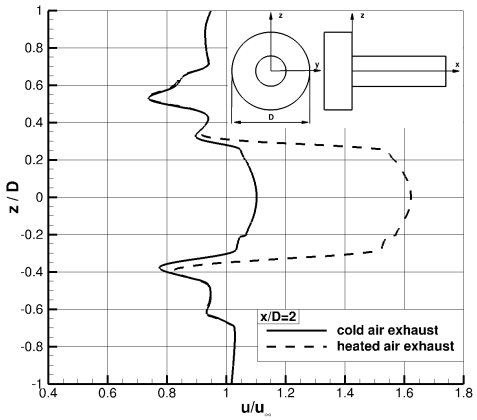

FIGURE 11. Velocity ratio $u/u\infty$ distribution behind the nozzle exit ($x/D = 2$) in the symmetry plane.

behind the nozzle exit ($x/D = 1.2$) at the axial position $x/D = 1.4$. The mixing region is in between the jet barrel shock and the outer compression shock (seen at $z/D = -0.5$). This mixing region divides the jet flow from the outer flow. The jet velocity in the center is for the heated air plume $47\ \%$ higher than for cold air. Note that the velocity variation at around $z/D = \pm 0.13$ is caused by the expansion fan at the nozzle lip. At $z/D = -0.25$, the width of the mixing area appears increased with the heated air plume, hence affective flow entrainment into the plume. Figure 11 shows the velocity ratio u/u_∞ in the symmetry plane further downstream at the axial position $x/D = 2$. The jet mixing layer is enlarged. It is now located between $z/D = -0.28$ and $z/D = -0.40$. At this position, the width of the heated jet mixing layer is about 1.7 times larger than for the cold jet which again indicates an effect on outer flow entrainment.

5. Conclusions

Heated jet computations for a generic rocket shape at $Ma = 3$ and first flow analyses are shown. The helium jet computations are not done yet. For the air jet the computed flow fields upstream the base are similar. The different total jet temperatures influence the afterbody flow and the flow downstream the nozzle. The influence of the jet temperature on pressure coefficient at the rocket base and at the nozzle fairing is shown. Also the influence on turbulent jet mixing behind the nozzle exit is shown. A significant change in mixing layer width is found which should result in a different entrainment of the outer flow. For an overview of the flow topology this Reynolds-Averaged Navier-Stokes equations (RANS) simulation are sufficient. For further afterbody flow analyses there is an unsteady solution necessary. For this approach are unsteady Reynolds-Averaged Navier-Stokes equations (URANS) simulations or Large Eddy simulations (LES) necessary. In future work we will compare these computations to experimental results.

Acknowledgments

Financial support has been provided by the German Research Foundation (Deutsche Forschungsgemeinschaft – DFG) in the framework of the Sonderforschungsbereich Transregio 40. Computational resources have been provided by the Leibniz-Rechenzentrum (LRZ) in Munich.

References

[1] PETERS, W. L. AND KENNEDY, T. L. (1979). Jet Simulation Techniques - Simulation of Aerodynamic Effects of Jet Temperature by Altering Gas Compositions. *AIAA-1979-327*.

[2] PETERS, W. L. AND KENNEDY, T. L. (1977). An Evaluation of Jet Simulation Parameters for Nozzle/Afterbody Testing at Transonic Mach Number. *AIAA-1977-106*.

[3] KUMAR, R. AND VISWANAH, P. R. (2002). Mean and Fluctuating pressure in Boat-Tail Separated Flows at Transonic Speeds. *Journal of Spacecraft and Rockets*, **39**(3).

[4] REIJASSE, P. AND DELERY, J. (1991). Experimental Analysis of the Flow past the Afterbody of the Ariane 5 European Launcher. *AIAA-91-2897*.

[5] STEPHAN, S., MÜLLER-EIGNER, R. AND RADESPIEL, R. (2013). Jet Simulation Facility using the Ludwig Tube Principle. *5th European Conference for Aeronautics and Space Sciences*.

[6] PINDZOLA, M. (1963). Jet Simulation in Ground Test facilities. *AGARDograph*, **79**(11).

[7] FREY, M. (2009). Personal communication. EADS Astrium.

[8] OSSWALD, K., HANNEMANN, V., HANNEMANN, K., STEPHAN, S. AND RADESPIEL, R. (2013). Numerical and Experimental Investigations of a Generic Rocket Launcher Configuration with Cold Plume in Hypersonic Flow. *5th European Conference for Aeronautics and Space Sciences*.

[9] YOU, Y., OSSWALD, K. AND HANNEMANN, V. (2012). Numerical Simulation of a Generic Rocket Base Flow with Plume in a Supersonic Environment. *SFB/TRR 40 – Annual Report 2012*.